Low CyaA expression and anti-cooperative binding of cAMP to CRP frames the scope of the cognate regulon of Pseudomonas putida

Arce-Rodríguez, Alejandro; Nikel, Pablo I.; Calles, Belén; Chavarría, Max; Platero, Raúl; Krell, Tino; de Lorenzo, Victor

Published in:
Environmental Microbiology

Link to article, DOI:
10.1111/1462-2920.15422

Publication date:
2021

Document Version
Peer reviewed version

Anti-cooperative binding of cAMP to the CRP regulator of *Pseudomonas putida* endows the regulon with a distinct *in vivo* functionality

by

Alejandro Arce-Rodríguez[1], Pablo I. Nikel[2], Belén Calles[3], Max Chavarría[4], Raúl Platero[5], Tino Krell[6] and Victor de Lorenzo[1*]

[1]*Department of Molecular Bacteriology, Helmholtz Centre for Infection Research, Braunschweig 38124, Germany.* [2]*The Novo Nordisk Foundation Center for Biosustainability, Technical University of Denmark, 2800 Kongens Lyngby, Denmark.* [3]*Systems Biology Department, Centro Nacional de Biotecnología-CSIC, Campus de Cantoblanco, Madrid 28049, Spain.* [4]*Escuela de Química, Universidad de Costa Rica, San José 2060, Costa Rica.* [5]*Departamento de Bioquímica y Genómica Microbianas, Instituto de Investigaciones Biológicas Clemente Estable, MEC, Montevideo, Uruguay.* [6]*Department of Environmental Protection, Estación Experimental del Zaidín CSIC, Granada 18008, Spain*

Originality-Significance Statement. One of the general rules of comparative genomics is that DNA sequence similarity between two given genes implies functional similarity as well. The cAMP-CRP system was one of the first regulatory devices studied in *E. coli* and its key role as a central regulatory device of metabolic transactions in this bacterium has been broadly demonstrated. It is thus tempting to assign the same function to the corresponding genes when found in other bacterial species. Surprisingly, the genome of the soil bacterium *Pseudomonas putida* encodes the same regulatory parts of the cAMP/CRP system of *E. coli* but its physiological role is altogether alien to metabolic control. In this article we provide a mechanistic basis for such a functional shift, that ultimately stems from the affinities that rule cAMP-CRP binding in *P. putida.* On this basis, we argue that the specific role of a given genetic device depends not only of the intrinsic properties of its components and their connections, but most importantly, of the parameters that control dynamic interplay among them.

* **Correspondence to:** Víctor de Lorenzo, Centro Nacional de Biotecnología (CNB-CSIC) Campus de Cantoblanco, Madrid 28049, Spain. Tel.: 34-91 585 45 36. Fax: 34-91 585 45 06. E-mail: vdlorenzo@cnb.csic.es

SUMMARY

Although the soil bacterium *Pseudomonas putida* KT2440 bears a *bona fide* adenylate cyclase gene (*cya*A) intracellular concentrations of cAMP are barely detectable. By using a battery of reporter systems and direct quantification of cAMP under various conditions, we show that such low levels of the molecule stem from the stringent regulation of its synthesis, efflux and degradation. Poor production of cAMP resulted both from the low catalytic activity of CyaA and inefficient translation of its mRNA. Moreover, inactivation of the cAMP-phosphodiesterase *pde* gene led to intracellular accumulation of the cyclic nucleotide, exposing an additional source of cAMP drain *in vivo.* But even with such low levels of cAMP, *P. putida* sustained a perfectly active cAMP signaling pathway that propagates into a large regulon. Genetic and biochemical evidence indicated that such phenomenon ultimately resulted from the unusual binding parameters of cAMP to CRP. This included an ultratight cAMP-Crp$_{P.\ putida}$ affinity (K_D of 45.0 ± 3.4 nM) and an atypical 1:1 effector/dimer stoichiometry that obeyed to an infrequent anti-cooperative binding mechanism. It thus seems that keeping the same regulatory parts and their relational logic but changing the interaction parameters enables genetic devices to take over entirely different domains of the functional landscape.

Keywords: *Pseudomonas putida*, cAMP, Crp, Adenylate Cyclase, cAMP-phosphodiesterase, metabolism, negative cooperativity

---

Since discovery of cAMP, this metabolite has been recognized as a universal second messenger due to the myriad of regulatory roles that it plays in virtually all kingdoms of life (Gancedo, 2013). This is in part due to its rapid turnover, which is tightly controlled by its rate of synthesis from ATP by the enzyme adenylate cyclase (AC) and/or its efflux and hydrolysis by specific cAMP-phosphodiesterases (PDEs) (McDonough and Rodriguez, 2011). In bacteria, cAMP was originally described in *E. coli* and shortly after it was linked to the control of carbon catabolite repression or CCR (i.e. the mechanism by which bacteria employ preferentially one carbon source in respect to others; Makman and Sutherland, 1965; Ullmann and Monod, 1968). Currently, it is accepted that CCR in enterobacteria is controlled by the rate of cAMP synthesis catalyzed by the AC. In the presence of a preferred carbon source (such as glucose), the carbohydrate is phosphorylated and transported inside the cell by the EIIA enzyme of the

phosphoenolpyruvate-carbohydrate phosphotransferase system (PTS), in order to be consumed by the glycolytic pathway. When glucose is exhausted, the phosphorylated EIIA enzyme accumulates in the cytoplasm and stimulate the enzymatic activity of the AC (Deutscher, 2008). The changes in intracellular cAMP levels are then perceived by the cAMP-receptor protein (Crp) trough allosteric interaction with its N-terminal cNMP binding domain. The interaction with cAMP triggers a series of conformational changes in this transcriptional factor that enable its C-terminal DNA recognition domain to activate the transcription of hundreds of genes (many of them directly involved in the utilization of non-preferred carbon compounds) (Shimada et al., 2011; Seok et al., 2014).

Owing that much of the initial research on cAMP was done in *E. coli*, it was typically assumed that the role of this molecule is always related to the control of differential carbon source consumption in bacteria. However, this paradigmatic vision has changed during the last years due to many studies that expanded the functions regulated by cAMP-Crp, relegating the control of CCR almost exclusively to enterobacteria. These traits include the control of basic metabolic adaptations such as biofilm formation (Hufnagel et al., 2016), motility (Fahrner and Berg, 2015), survival to oxidative stress (Molina-Quiroz et al., 2018) or the CRISPR/Cas antiviral defense mechanism (Yang et al., 2020). Moreover, in important pathogenic bacteria such as *Klebsiella pneumoniae*, *Vibrio cholerae* or *P. aeruginosa*, the Crp-cAMP homologue systems regulate the transition between virulent and avirulent behaviors (McDonough and Rodriguez, 2011; Xue et al., 2016). This diversification of functions for the same regulatory system in many bacteria exhibit an evolutionary mechanism through which regulons governed by the same transcription factor can dramatically diversify in different hosts, in a clear example of regulatory exaptation at molecular level (Milanesio et al., 2011).

Pseudomonas putida is a ubiquitous bacterium that could be found colonizing soil, rhizosphere and water environments. Over the last years, this bacterium has been renowned as a robust *chassis* for industrial biocatalysis processes, due to its remarkable versatile metabolism, its high tolerance to toxic compounds, and the wealth of genetic tools available for genomic engineering (Nikel and de Lorenzo, 2018). Much of the biotechnological interest on *P. putida* stems from the distinct architecture of its central carbon metabolism when compared to other microbes. These differences allow the bacterium to produce a high concentration of NAD(P)H to cope with redox-intensive reactions (Nikel et al., 2015; Akkaya et al., 2018). Along with the differences in central metabolism, the preferential utilization of carbon

compounds in *P. putida* also differs significantly compared to other microorganisms. Interestingly, neither variations in the intracellular cAMP (Phillips and Mulfinger, 1981; Rojo, 2010), nor the mutation of *crp* or *cya*A genes altered significantly the gross metabolic profiles in this bacterium (Milanesio et al., 2011). These observations rule out the possibility that either cAMP or $Crp_{P.\ putida}$ plays a role in the control of CCR. Conversely, the preferential selection of carbon sources in *P. putida* seems to be governed by a sophisticated posttranscriptional mechanism that involves the interaction of sRNA antagonists, the catabolite repression control protein Crc and the RNA binding protein Hfq (Moreno et al., 2015). Moreover, some CCR-unrelated functions orchestrated by cAMP-Crp in *P. putida* have been recently reported. These features include the utilization of various amino acids (such as phenylalanine) or dipeptides as nitrogen sources, or the resistance to a small number of bactericidal agents (Milanesio et al., 2011; Herrera et al., 2012). More recently, (Xiao et al., 2020) showed that $Crp_{P.\ putida}$ directly represses the expression of *gcs*A (a novel diguanylate cyclase involved in the repression of swimming motility) in a cAMP dependent manner.

In addition to its regulatory duties, another puzzling aspect of cAMP-$Crp_{P.\ putida}$ is the mechanistic of Crp activity. As it has been shown, *P. putida* maintains its cAMP concentrations remarkably low regardless of its growth conditions (Arce-Rodriguez et al., 2012). Nevertheless, $Crp_{P.\ putida}$ activation by cAMP is ultimately required to trigger the transcription of its cognate promoters (Milanesio et al., 2011). Hence, how is possible to hold an active cAMP-Crp system with such limited effector concentrations and which mechanisms are used by *P. putida* to keep the cAMP at bay? In this work we have explored these issues and we have found that *P. putida* has adapted its entire cAMP-Crp regulatory system to function with extremely short amounts of the effector. This low intracellular cAMP pool is maintained by controlling every step of cAMP-production, from the expression of its unique AC to the degradation and excretion of the metabolite outside the cell. By the titration of cyclic nucleotides to the apo-$Crp_{P.\ putida}$, we finally show that this transcriptional factor is able to detect such extremely low amounts of cAMP due to its extremely high affinity for the metabolite and its unique 1:1 effector/dimer stoichiometry.

RESULTS

PP_4917 encodes a putative 3',5'-cyclic-AMP *phosphodiesterase*

As we have previously described, the genome of *P. putida* KT2440 encodes singular orthologues of one class I adenylate cyclase (*cya*A) and the cAMP receptor protein (*crp*) (Milanesio et al., 2011). Additionally, a protein encoding a class III cAMP-phosphodiesterase (CpdA) was characterized in its closely relative *P. aeruginosa* as being responsible for the degradation of cAMP (Fuchs et al., 2010). We therefore sought out for a homolog of this protein in the genome of *P. putida* using BLASTP. Only one protein of 266 aa residues resulted to be highly similar to $CpdA_{P.\ aeruginosa}$, with 54% identity and 69% similarity. This positive match is encoded by the gene locus PP_4917, which was previously annotated as Icc protein (Nelson et al., 2002). However, after the last update of *P. putida* KT2440 genome (Belda et al., 2016) the gene was renamed as *pde,* which stands for 3',5'-cyclic-nucleotide phosphodiesterase. The genomic location and expression profile of PP_4917 is shown in Fig. 1A. To get further insights into the function of PP_4917 product, its amino acid sequence was aligned with the sequence of five previously described cAMP-phosphodiesterases from bacteria. The alignment showed that *P. putida* PP_4917 preserves all the 13 residues that are absolutely conserved among class III phosphodiesterases (Supplementary Fig. S1). Unlike *crp* and *cya*A, that are transcribed as stand-alone genes (Fig. 1B and 1C), the *pde* genomic context could enable this gene to be co-transcribed as part of a large polycistronic mRNA along with other important genes like *par*C and *par*E, encoding the A and B subunits of a type IV DNA topoisomerase, respectively (Fig. 1A). However, the levels of transcription of *pde* were found to be considerably lower than those of the rest of its surrounding genes, regardless of the carbon source used for bacterial growth (Fig. 1A). This result suggests that *P. putida pde* could also be expressed independently of its genomic context in a similar fashion as *crp* and *cya*A (Fig. 1B, 1C). Next, in order to verify the activity of Pde as a genuine 3',5'-cyclic-AMP phosphodiesterase, we investigated whether the loss of *pde* affected the intracellular accumulation of cAMP.

Inactivation of pde *gene increases the transcriptional activation of cAMP-Crp dependent promoters*

A reporter system was designed to correlate the intracellular levels of cAMP with the fluorescence produced by the GFP protein expressed through a $P_{CC\text{-}41.5}$ synthetic promoter (Gaston et al., 1990). This correlation is achieved since transcription from $P_{CC\text{-}41.5}$ is dependent on the activation by the cAMP-Crp complex through a class II Crp-activation mechanism (Busby and Ebright, 1999). The reporter system (which is carried in plasmid pCAMPS, Table 1) was transformed into wild-type *P. putida* KT2440 and into its *crp*, *cya*A and *pde* mutants. As stated above, cAMP production (and therefore Crp activity) in *E.*

coli is tightly linked to carbon consumption via the CCR mechanism (Deutscher, 2008). Although the Crp-cAMP system of *P. putida* seems to be independent of carbon source consumption (Milanesio et al., 2011), we sought out whether different metabolic regimes could affect the activation of the cAMP sensor. Thus, the strains bearing pCAMPS plasmid were grown in M9 minimal medium with either glycolytic or gluconeogenic carbon sources and the GFP fluorescence produced was recorded along the growth curve. Fig. 2 shows the relative GFP fluorescence measured in exponential and stationary phase of growth. Noteworthy, the fluorescence levels in the wild-type strain KT2440 were very similar regardless of the carbon source used for growth. This result reaffirms our previous findings that the Crp-cAMP system is not linked with carbon consumption in *P. putida* (Milanesio et al., 2011). We also noticed that in both Δ*cya*A and Δ*crp* mutants the intensity of GFP was significantly lower than in the wild-type strain in all the carbon sources tested, which reflects the activation of the synthetic promoter by the cAMP-Crp complex. Fig. 2 also shows the GFP fluorescence in the *pde* transposon mutant. We expected that, if Pde is an authentic cAMP-phosphodiesterase, the intracellular pool of this metabolite in the mutant should increase. With higher cAMP levels, the amount of cAMP-activated Crp would also raise and therefore it will produce an increment in the transcription of cAMP-Crp activated promoters such as $P_{CC\text{-}41.5}$. This was indeed the case when cells were grown in sugars (glucose and fructose) as carbon and energy sources. No significant difference was observed when cells were grown in succinate, suggesting that Pde activity might be itself subject to metabolic control.

P. putida retain very low cAMP levels

To correlate the genetic data above with the actual cAMP available *in vivo* to the cognate regulatory device we developed a sensitive HPLC-ESI-MS analytical procedure to test and quantify the levels of this cyclic nucleotide both in the culture supernatant and the cytoplasm of bacteria grown in different media (see Experimental procedures). Note that the quenching method was adapted for full recovery of the analyte at the moment of cell harvest. As control of sensitivity for this method, equivalent samples of wild-type and *cya*A strains of *E. coli* were also processed. It is noteworthy that *E. coli* wild type was cultured in conditions where it is expected to produce high amounts of cAMP (Joseph et al., 1982). Conversely, the Δ*cya*A strain of *E. coli* was cultured in 0.2% (w/v) glucose since it fails to grow on succinate as carbon source. The results of these experiments are shown in Fig. 3A. As anticipated, cAMP was found both intracellularly (~2.5 μM) and in the external medium (~16 μM) of cultures of the

wild-type *E. coli* strain. In contrast, cAMP was not detected in the *cya*A strain, a result that was expected for a mutant in the sole adenylate cyclase of this bacterium. The same procedure was then applied to *P. putida* KT2440 and its *cya*A and *pde* mutants while growing on succinate or glucose. In contrast to *E. coli,* we were unable to detect the metabolite in *P. putida* cells collected and processed with the same protocol (Fig. 3B and 3C, left panels). While earlier genetic data suggested cAMP levels in *P. putida* to be very low (Phillips and Mulfinger, 1981; Milanesio et al., 2011; Arce-Rodriguez et al., 2012), we wondered how the *cyaA* gene (and thus production of cAMP) was required to activate the $P_{CC\text{-}41.5}$ – *GFP* fusion borne by pCAMPS (Fig. 2) without any detectable production of cAMP, at least with the level of sensitivity of our analytical method. One possibility is that cAMP is indeed produced but the levels are so low that they scape the HPLC-ESI-MS technology adopted. This may stem from a very low activity of CyaA or a very high activity of Pde—or both. To shed some light on this matter, we turned our attention to the determinants of *cyaA* expression as a way to artificially increase cAMP production

The cya*A gene of P. putida is transcribed, but not efficiently translated in* P. putida

Quantification of cAMP (Fig. 3B and 3C, left panels) confirmed that *P. putida* cells produce undetectable levels of the cyclic nucleotide, even when the Pde phosphodiesterase gene was disrupted. This low cAMP production could be caused *inter alia* by a deficient enzymatic activity of the adenylate cyclase itself, but also due to low transcription/translation rates of the *cya*A. Genome-wide transcriptomic analysis of *P. putida* performed by our group and by others (Yuste et al., 2006) have shown that the adenylate cyclase specific mRNA is efficiently transcribed regardless of the growth conditions (Fig. 1C). On the other hand, close examination of *P. putida* 5' UTR of *cya*A mRNA revealed that the putative Shine-Dalgarno (SD) motif of this gene is suboptimal according to the GGAGG nucleotide core that interacts directly with the anti-SD sequence of the 16S rRNA ((Ma et al., 2002); Supplementary Fig. S2). The absence of a good quality SD could inhibit proper formation of the translation initiation complex, preventing the efficient translation of *cya*A mRNA into the adenylate cyclase enzyme. To test this hypothesis, two plasmid-borne translational (pARPcyaA1) and transcriptional (pARPcyaA2) fusions of the $cyaA_{P.\ putida}$ promoter (P_{cyaA}) were constructed in frame with the *lac*Z gene (Table 1). The initial quantification of *cya*A'-'*lac*Z translational fusion activity was performed by the classical β-galactosidase assay described by Miller (Miller, 1972). Nonetheless, the values obtained were too low to be significant for this method (i.e. <15 Miller Units, results not shown). Therefore, we resorted to the ultra-sensitive

Galacto-Light Plus™ commercial system. Fig. 4A shows the corresponding LacZ activity for both translational and transcriptional fusions of P_{cyaA}, measured in *P. putida* KT2440, Δ*crp* and Δ*cya*A strains grown on different carbon sources (succinate, glucose, fructose). The results reveal a remarkable difference amongst the transcription and the translation levels of the *cya*$A_{P.\ putida}$ gene, the transcriptional activity of the promoter being between 10-30 fold-change higher than the translational activity in the conditions tested. As observed, neither deletion of *crp* nor *cya*A genes affect the activity of the P_{cyaA}, conversely to *E. coli* where the cAMP-Crp complex repress *cya*$A_{E.coli}$ expression trough binding to the P2 promoter of the gene (Aiba, 1985; Mori and Aiba, 1985). This result was confirmed by an electrophoretic mobility shift assay (EMSA) of a ~200 bp end-labeled DNA fragment comprising the upstream region of *cya*$A_{P.\ putida}$ gene and purified $Crp_{P.\ putida}$. Even at protein concentrations as high as 5 μM, $Crp_{P.\ putida}$ was not able to retard noticeably the electrophoretic migration of the P_{cyaA} DNA probe despite of the presence of cAMP (not shown).

Besides the translation initiation bottleneck of CyaA just described, we noticed also that the codon usage through the gene was clearly suboptimal, what could surely add to a poor expression of the signal. To overcome this state of affairs we reconstructed a fully synthetic version of $CyaA_{P.\ putida}$ that maintained the primary amino amino acid sequence but with translation signals, codon usage and other features optimized for a better expression of the enzyme (see Experimental procedures and Supplementary Fig. S3).

Pde phosphodiesterase contributes to the low levels of cAMP in P. putida

To validate the enhanced *cya*A version described above (Supplementary Fig. S3; named hereafter as *cya*A-GA), its activity was first tested in *E. coli.* To this end, its coding sequence was cloned under the control of *lacI*^{q}-P_{trc} of pVTR-A (Table 1), and the NotI fragment from this vector passed to the broad host range plasmid pSJ33 (Table 1), thereby generating pARC5. This plasmid, along with control constructs pARC2 (encoding *cya*A of *E. coli*) and pMZC5 (expressing native *cya*A from *P. putida*) were transferred into the *E. coli* mutants W3110 *cya*A and the cAMP-hypersensitive TP610A strain (Crasnier and Danchin, 1990). Transformed cells were plated onto MacConkey agar to observe the complementation of the maltose utilization phenotype. As shown in Fig. 5, only the optimized *cya*A-GA gene was able to partially restore the consumption of maltose (red colonies) when it was transformed into *E. coli* W3110 *cya*A and

cultured in presence of IPTG (Fig. 5 panel 3). On the other hand, native *cya*A$_{P. putida}$ failed to restore this phenotype regardless of the presence of the inducer (Fig. 5 panel 2). This observation was even more evident when both plasmids were transferred to the cAMP-hypersensitive strain TP610A. In this case, the native *cya*A from *P. putida* was able to complement the maltose utilization phenotype in the *E. coli* host, but exclusively when it was overproduced by the addition of IPTG (Fig. 5, panel 5). Conversely, overexpression of *cya*A-GA was not necessary to complement the maltose phenotype (Fig. 5, panel 6). Moreover, overproduction of *cya*A-GA by IPTG resulted to be toxic for strain TP610A.

Once the cyclase activity of the refactored *cya*A-GA gene product was verified, the cognate DNA sequence was cloned anew into pSEVA424 (Table 1), transformed into *P. putida* strains Δ*cya*A and *pde*$^{-}$, and its cAMP levels measured both intracellularly and in the extracellular medium with the same protocol described above. In this case, a clear boost of cAMP production was observed in cultures of *P. putida* bearing the pARC5 plasmid (Fig. 3B and C, right panel). Similarly as in *E. coli*, cyclic-AMP was mainly present in the culture supernatants of *P. putida,* reflecting a process in which cAMP is efficiently transported outside the cell. Importantly, we observed that cAMP concentrations were significantly higher in the *pde*$^{-}$ mutant compared to wild type *P. putida* KT2440, in both succinate and glucose. The results of Fig. 3B and 3C (right panels), together with the homology studies of *pde* (Supplementary Fig. S1) and the observation that GFP fluorescence produced by $P_{CC-41.5}$ increase in the *pde*$^{-}$ strain (Fig. 2), confirm that [i] the CyaA protein is a perfectly functional cAMP cyclase, [ii] the low levels of the cyclic nucleotide in *P. putida* can be traced to a very poor translation of the *cya*A mRNA and [iii] Pde is a functional and genuine cAMP-phosphodiesterase that further helps to keep cAMP levels low.

Influence of extracellular cAMP in the activation of $P_{CC-41.5}$-GFP synthetic reporter

Due to the previous observation that cAMP was accumulated in the extracellular cultures of both *P. putida* and *E. coli* (compared to the intracellular milieu), the next step was to analyze whether the cyclic nucleotide could be transported back to the cytoplasmic space. First, the ability of an *E. coli cya*A deficient strain to grow in maltose as sole carbon sink was assessed upon addition extracellular cAMP. In normal conditions, a *cya*A-deficient *E. coli* is unable to metabolize this carbon source due to the lack of Crp activation. However, the amendment of high concentrations (i.e. 100 μM-1mM) of cAMP to the culture medium restored the growth in maltose, indicating that *E. coli* is able to uptake and use external

cAMP (Fig. 6A). Next, we examined the cAMP-Crp dependent activation of the $P_{CC-41.5}$ synthetic promoter by exogenous cAMP. In order to do so, *E. coli* W3110 *cya*A strain was transformed with plasmid pCAMPS and production of GFP fluorescence was monitored in the absence and in the presence of different cAMP concentrations. As shown in Fig. 6B (left panel), GFP signal strongly increased upon addition of cAMP. Furthermore, the fluorescence increase was proportional to the amount of cAMP added, confirming that *E. coli* efficiently sense the effector present in the extracellular milieu.

Following this, the reporter plasmid pCAMPS was transformed into *P. putida* KT2440 strain and its Δ*cya*A derivative in order to analyze its behavior. Cells were grown in equivalent conditions as those used in the previous experiments with *E. coli* to record the GFP fluorescence as an indicator of cAMP uptake. In a similar fashion as observed in the experiments with *E. coli*, the GFP intensity was significantly lower in the *cya*A deficient strain of *P. putida* compared to its wild-type counterpart (see Fig. 6B, right panel). However, in this case addition of cAMP did not affect GFP fluorescence even at concentrations as high as 1 mM, suggesting that—contrary to *E. coli* bacterium— *P. putida* is neither permeable to cAMP, nor able to actively internalize extracellular cAMP at least in the conditions tested.

$Crp_{P.putida}$ binds one cAMP molecule per protein dimer

We have shown previously that $Crp_{P.putida}$ is a dimeric protein, which undergoes a strong conformational change upon tight binding of cAMP (Arce-Rodriguez et al., 2012). Regardless of the high quality of these results, some aspects of this interaction remain ambiguous. This previous work showed that an MBP-$Crp_{P. putida}$ fusion protein binds cAMP with an overall stoichiometry of approximately 0.65, which is close to 0.5 (i.e. 1 molecule of cAMP per dimer of Crp) and occurred in a single binding event, describing a monophasic curve (Arce-Rodriguez et al., 2012). This is an important outcome to take into account, because all the Crp-like proteins described so far bind two or more cyclic nucleotides per protein dimer (Weber and Steitz, 1987; Passner and Steitz, 1997; Stapleton et al., 2010; Cordes et al., 2011; Townsend et al., 2014). One of the hypotheses to explain this odd stoichiometric value is the ultratight affinity of $Crp_{P. putida}$ for cAMP (KD = 22.5 ± 2.8 nM). This strong interaction could cause the carryover of cAMP (either produced by *E. coli* or present in the culture medium) that is still interacting to MBP-$Crp_{P. putida}$ during protein purification. Therefore, we decided to modify the purification protocol and

pursued to overexpress the MBP-Crp$_{P.putida}$ fusion protein in a *E. coli* W3110 Δ*crp* Δ*cya*A strain grown in M9-glucose medium in order to obtain a Crp$_{P.putida}$ devoid of any source of cAMP (see Experimental procedures). Also, the ITC reaction buffer was also optimized by increasing concentrations of KCl to 250 mM and by adding DTT at 1 mM, in order to sustain a reducing *milieu* for the 6 cysteine residues of the protein. Altogether, these modifications allowed us to conduct the ITC experiments again with a >95% pure, cAMP-less Crp cleaved from MBP (apo-Crp$_{P.putida}$).

Fig. 7A shows the titration of apo-Crp$_{P.putida}$ with cAMP. The hyperbolic curve traced from plotting the titration data is virtually identical to the one observed previously for MBP-Crp$_{P.putida}$ (Arce-Rodriguez et al., 2012), the binding being driven by favorable changes in the enthalpy (Δ*H*) and entropy (*T*Δ*S*) of the system (Table 2). Likely, the interaction between both molecules yields once again a tight binding for the cyclic nucleotide (K_D = 45 ± 3 nM). In spite of these similarities, the affinity for the cyclic nucleotide in the apo-protein is somewhat reduced as compared to the fusion protein (Table 2). However, this minor discrepancy is likely to be caused by the increment in the ionic strength to 250 mM KCl and not by the absence of the MBP tag. Moreover, integration of data with the *One Binding Site* model results in a very satisfactory fit, which describes only one binding event and confirms without any doubt the stoichiometry of 1 molecule of cAMP per dimer of Crp$_{P.putida}$. This reflects a scenario in which only one of the (at least) two cAMP binding sites available in the protein becomes occupied.

Similarly, the titration of apo-Crp$_{P.putida}$ with cGMP plotted in Fig. 7B was very similar to the interaction of the cyclic nucleotide for the MBP fusion protein (Arce-Rodriguez et al., 2012). Nevertheless, in this case the binding of cGMP is driven by negative entropy changes (Table 2). This unfavorable Δ*S* value can have different reasons and is not necessarily caused by an ordering of water molecules at the complex interface. Another important negative contribution to the entropy change is the loss of flexibility of the ligands during the binding process (Jelesarov and Bosshard, 1999). Thus, the cGMP-Crp$_{P. putida}$ complex could occur in a way where the interaction process does not alter the conformational architecture of the binding sites and therefore, the entropy of the system is negative. The affinity of the cGMP for apo-Crp$_{P.putida}$ is ~100 fold lower than the one observed for cAMP with the same protein. Furthermore, as was the case with cAMP interaction for apo-Crp$_{P.putida}$, there is just one binding event for cGMP-Crp$_{P.putida}$ complex. Despite the less defined shape of the ITC plot, the *One Binding Site* model fitting of the data yields again a binding stoichiometry closer to 0.5 (0.327 ± 0.084, Table 2), which is

consistent with the model proposed that only one molecule of the cyclic nucleotide (cAMP or cGMP) is interacting with the $Crp_{P.putida}$ dimeric protein.

DISCUSSION

We show above that—similarly to *E. coli* and many other bacteria— *P. putida* does have a complete regulatory device that encompasses transcriptional regulator CRP its cognate effector cAMP and the two enzymes that dynamically regulate the levels of this signaling molecule: AMP cyclase CyaA and the phosphodiesterase Pde[1]. the Yet, the actual levels of cAMP borne by *P. putida*, while still retaining their regulatory effects are extremely low. The results shown in this work document that such low levels are the result of the very poor synthesis of cAMP (plausibly due to the equally low down translation of CyaA, its degradation, the efflux to the extracellular milieu and the lack of transport back to the cells. This shortage of cAMP is compensated by the extraordinary affinity of $Crp_{P.putida}$ for the second messenger. In addition, the results document one single event of cAMP binding to a $Crp_{P.putida}$ dimer, i.e. a stoichiometry of 0.5 or occupancy of just one monomer of the functional protein dimer. This figure differs notably in respect of what is known for $Crp_{E.\ coli}$, where effector/monomer ratios are 1:1 (Weber and Steitz, 1987) if not higher (Gorshkova et al., 1995; Passner and Steitz, 1997; Lin and Lee, 2002). Yet, the ITC data of Fig. 7 shows that only one of the two cAMP binding sites available in the dimer becomes occupied. Binding of one effector molecule to one of the subunits of the dimer thus appears to decrease affinity of the corresponding site in the other subunit in sort of *negative cooperativity*. A similar behaviour was observed when binding experiments were repeated with cGMP (Fig. 7B). While overall affinity for this effector was lower, the results fitted a stoichiometry close to 0.5 (0.327 ± 0.084, Table 2), which would indicate binding of a single molecule per dimer i.e. cGMP is also likely to interact with $Crp_{P.\ putida}$ through the same process as cAMP. Counter-intuitive as it may look, *negative cooperativity* has been observed in other proteins (Milligan and Koshland, 1993; Teran et al., 2006), including to $Crp_{E.\ coli}$, where cAMP binding seems to involve a negative allosteric interaction in the sequential interplay of the effector to its binding sites. Yet, the second cAMP binding event to the non-occupied $Crp_{E.\ coli}$ monomer is possible because of the high intracellular level of the effector in this bacterium, what restores dimer symmetry (Popovych et al., 2006; Rodgers et al., 2013; Seok et al., 2014; Townsend et al., 2015). In

[1] A detailed analysis of each of the Results presented in this article can be found in the Supplementary Materials *on line.*

contrast, the intriguing possibility that the cAMP-bound $Crp_{P.putida}$ is not symmetric owing to partial occupancy of the dimer opens the possibility that the regulator may recognize non-palindromic DNA sequences—an issue that deserves further studies. This state of affairs is quite different of that found in other bacteria that have the same regulatory players. For instance, *P. aeruginosa* has two 2 ACs (Topal et al., 2012) one of them membrane-bound and clearly controlling cAMP levels for regulation of the Crp homologue Vfr, which in turn rules expression of a suite of virulence genes (Coggan and Wolfgang, 2012). Another remarkable case of unusual Crp/cAMP system is that of *Mycobacterium tuberculosis*. The device borne by this bacterium included at least 16 AC-like proteins (Stapleton et al., 2010; Green et al., 2014) and (in sharp contrast with P. putida) includes a Crp protein with a low affinity for cAMP to compensate the much higher levels of cAMP produced by the many ACs (Green et al., 2014). In between we find the canonical Crp protein of *E. coli*, which possesses a mid-sensitive avidity for cAMP (REF) compared to the *P. putida* or the *M. tuberculosis* counterparts.

The obvious question elicited by the diversity of parameters that rule the interplay Crp-cAMP-cyclase(s)-phosphodiesterase(s) is the biological and evolutionary logic of such a remarkable range of specific values. These make the system to keep the same molecular actors and behave mechanistically the same but delivering quite different transfer functions between the inputs and the outputs of the regulatory device. One revealing detail in this respect is the apparently paradoxical expression of the *cyaA* gene of *P. putida* (Fig. 1C and Fig. 4). While transcription initiation of this gene is well detectable, translation seems to be very poor owing to a bad SD motif in its 5'-UTR and a non-optimal codon usage through the coding sequence. Unbalance of translational rates vs. transcription levels typically rule phenotypic variation generated by the noise in protein expression (Trotot et al., 1996). In the case of genes with low transcription but high translational rates, variations in mRNA synthesis result in strong stochastic fluctuations in protein concentration (Supplementary Fig. S4A). Conversely, a gene with high transcription and low translation produces smaller protein bursts that cause only week fluctuations in protein concentration, generating smaller phenotypic variation in the cell population (Supplementary Fig. S4B) (Ozbudak et al., 2002; Kaern et al., 2005). Inefficient translation of $cyaA_{P. putida}$ could thus be a a way to keep a low, non-fluctuating expression of CyaA, a situation that could benefit the environmental lifestyle of *P. putida.* On these bases, we entertain that keeping the same regulatory parts and their relational logic but changing the interaction parameters enables genetic devices to occupy entirely different domains of the functional landscape.

EXPERIMENTAL PROCEDURES

Strains, plasmids, and growth conditions

A description of the strains and plasmids employed in this work is summarized in Table 1. All *P. putida* derivatives were engineered from reference strain KT2440 (Nelson et al., 2002). A mini-Tn*5* insertion mutant in the locus PP_4917 (encoding the putative cAMP-phosphodiesterase Pde) was obtained from the *P. putida* KT2440 mutant library (Duque et al., 2007). The *E. coli* adenylate cyclase mutant W3110 *cya*A and the cAMP-hypersensitive strain TP610A were employed for *cya*A complementation assays (Milanesio et al., 2011). These experiments were performed in indicator plates prepared by adding maltose at 1.0% (w/v) to MacConkey agar base (Miller, 1972). Fermentation of maltose was detected by the appearance of red-colored colonies. *E. coli* strains CC118, DH5α and JM109 were used for routine maintenance of plasmids. Additionally, the replication of plasmids with oriR6K suicide replication origin (see Table 1) was carried out in *E. coli* DH5α*λpir*. Unless otherwise indicated, *P. putida* and *E. coli* cells were grown at 30°C and 37°C, respectively, in either rich LB medium or in synthetic mineral M9 medium (Sambrook et al., 1989) supplemented with the C-sources indicated in each case at 0.2% (w/v). Where necessary, media were amended with the following antibiotics to retain plasmids or to select for plasmid cointegration: ampicillin (Ap), 150 μg/ml for *E. coli* or 500 μg/ml for *P. putida*; chloramphenicol (Cm), 40 μg/ml; kanamycin (Km), 50 μg/ml; tetracycline (Tc), 8 μg/ml; streptomycin (Sm), 50 μg/ml; and gentamycin (Gm), 10 μg/ml.

Recombinant DNA and protein techniques

General methods for DNA manipulation were performed following standard protocols described elsewhere (Sambrook et al., 1989). Specific chromosomal segments of *P. putida* were amplified from ~100 ng of genomic DNA by means of polymerase chain reactions (PCR) in a buffer containing 1.5 mM $MgCl_2$, 0.2 mM of each deoxynucleoside triphosphate (dNTP), 0.5 μM of oligonucleotides and 1 U of GoTaq DNA polymerase (Promega, Madison, WI, USA). A list of the oligonucleotides used in this work is described in Supplementary Table S1. PCR reactions were run by an initial denaturalization 5 min at 94°C followed by 30 cycles of denaturalization (1 min, 94°C), annealing (1 min, 56°-62°C), extension

(1-3 min, 72°C) and one final cycle of extension (10 min, 72°C). Additionally, in PCR reactions carried out with high fidelity *Pfu* DNA polymerase (Promega, Madison, WI, USA), the extension temperature of reactions was increased to 75°C. In some cases, the same PCR reaction was directly run on a small amount of bacterial biomass picked from isolated colonies grown on agar plates. Amplified DNA segments were purified from PCR or agarose gels using the NucleoSpin Gel and PCR clean-up kit (Macherey-Nagel, Düren, Germany). Plasmid DNA was extracted from bacterial cells with the commercial Wizard® *Plus* SV Minipreps DNA Purification kit (Promega, Madison, WI, USA). The restriction endonucleases for DNA digestion and cloning were purchased from New England Biolabs (Ipswich, MA, USA) and used according to the manufacturer indications. Digested DNA was ligated by overnight incubation with T4 DNA ligase (Roche Applied Science, Mannheim, Germany) at 16°C. When necessary, PCR-amplified DNA fragments were verified by Sanger sequencing (Secugen SL, Madrid, Spain). The mobilization of plasmid DNA into *E. coli* cells was carried out by chemical transformation of cells prepared in CaCl2 solution (Sambrook et al., 1989), or by electroporation as described by Wirth *et al.* (Wirth et al., 1989). In the case of *P. putida*, plasmids were incorporated by conjugative triparental mating using *E. coli* HB101 (pRK600) as helper strain (de Lorenzo and Timmis, 1994) or by electroporation of cells previously washed and concentrated with 300 mM sucrose as indicated by Choi *et al.* (Choi et al., 2006).

Protein extracts were analyzed by denaturing-polyacrylamide gel electrophoresis (SDS-PAGE) in 10-15% (w/v) acrylamide/bisacrylamide (29:1) gel cast following standard procedures (Sambrook et al., 1989). Whole cells and proteins were resuspended in a denaturing buffer containing 60 mM Tris-HCl pH 6.8, 2% (w/v) sodium dodecyl sulfate (SDS), 5% (v/v) glycerol, 1% (v/v) β-mercaptoethanol and 0.005% (w/v) bromophenol blue, and boiled during 5 min prior to loading. At last, proteins were visualized by staining the gels in a solution containing 0.05% (w/v) of Coomassie R-250 blue dissolved in 50% (v/v) methanol and 10% (v/v) acetic acid.

Comparison of the aminoacidic sequence of bacterial cAMP-phosphodiesterases.

In order to find a putative cAMP-phosphodiesterase encoded in the chromosome of *P. putida*, the amino acid sequence of *P. aeruginosa* CpdA (Fuchs et al., 2010) was blasted against the non-redundant protein sequences from strain KT2440 using NCBI BLASTP version 2.2.28+

(http://blast.ncbi.nlm.nih.gov/Blast.cgi) (Altschul et al., 1997). Only a single protein of 266 aa encoded by locus PP_4917 resulted similar to CpdA$_{P.\ aeruginosa}$. Following, the aminoacid sequence of *E. coli* CpdA, *Haemophilus influenzae* Icc, *Mycobacterium tuberculosis* Rv0805, *Delftia acidovorans* PdeA and *Pseudomonas aeruginosa* CpdA (all of them encoding cAMP-phosphodiesterases) were retrieved from the NCBI database and aligned to the PP_4917 gene product from *P. putida* using the T-Coffee online server (http://www.tcoffee.org/) (Di Tommaso et al., 2011).

Construction of Δ*crp and* Δcya*A variants of* P. putida *and assembly of vectors to overexpress an optimized version of* cya*A*$_{P.\ putida}$ *gene*

The deletion of *crp* and *cya*A genes in *P. putida* was obtained by the seamless allelic replacement method described in Martínez-García and de Lorenzo (Martinez-Garcia and de Lorenzo, 2011). In the case of *crp*, the upstream and downstream flanking regions of the gene (~0.5 kb each) were PCR amplified respectively with primer pairs aacrpU-F/aacrpU-R and aacrpD-F/aacrpD-R. Both amplicons were linked in a single DNA segment by overlap extension (SOE)-PCR using primers aacrpU-F and aacrpD-R. The ensuing ~1 kb fragment was *EcoRI/SalI* digested and cloned within the same sites of pEMG, generating plasmid pARCrp9. Meanwhile, the upstream and downstream flanking regions of *cya*A (~0.5 kb each) were also PCR amplified with primer pairs aacyaAU-F/aacyaAU-R and aacyaAD-F/aacyaAD-R, and joined by (SOE)-PCR in a similar fashion. The ~1 kb DNA product was *EcoRI*/*BamHI* digested and ligated into the same sites of pEMG to construct plasmid pJΔcyaA for further deletion of *cya*A. Both suicide vectors were independently mobilized by conjugation to *P. putida* KT2440 already carrying pSW-1 (the latter plasmid encodes the expression of I-SceI endonuclease under the control of Pm promoter). The Km and Ap (500 μg/ml) resistant clones were selected and grown overnight in 2 ml of LB medium containing Ap and 15 mM 3-methylbenzoate to drive the expression of I-SceI. Next, induced cells were plated in LB-Agar, and checked for the resolution of the cointegrated plasmid by sensitivity to kanamycin in LB-Agar supplemented with the antibiotic. The Km sensitive clones were selected and tested by PCR to identify the accurate deletion of *crp* and *cya*A using primer pairs aacrpU-F/aacrpD-R and aacyaAU-F/aacyaAD-R, respectively. Finally, pSW-1 was diluted by three consecutive subcultures of cells in liquid LB. The loss of this plasmid was confirmed by sensitivity to ampicillin in LB-Ap plates. Additionally, a special collection of vectors was generated to enhance the synthesis of cAMP in *P. putida*. For this purpose, the entire *cya*A gene of this bacterium was chemically synthesized to

optimize the codon usage, to prevent AT-rich or GC-rich sequence stretches, to eliminate internal *cis*-acting sites (such as recombination sites or internal RBS sequences) and to avoid RNA secondary structures. Furthermore, a strong Ribosome Binding Site (RBS) was placed upstream of the start codon to enhance the translation of the gene, while two STOP codons were added at the end of the gene (Supplementary Fig. S3). The optimized *cya*A version (referred as *cya*A-GA from now on) was synthesized by Geneart (Life Technologies, Regensburg, Germany) with flanking *KpnI*/*SacI* sites into the cloning vector pGA15. In order to boost the expression of the optimized CyaA-GA, three expression vectors were generated as follows. First, *Kpn*I/*Sac*I restriction enzymes were used to clone *cya*A-GA into the same sites of plasmid pVTR-A, thus generating pARC1. This vector transcribes *cya*A-GA under the control of IPTG by P_{trc} promoter. The resulting *lacI*^{q}/P_{trc} → *cya*A-GA fragment from pARC1 was isolated afterwards as a single *Not*I segment and cloned into the low copy and broad host range vector pSJ33 to produce plasmid pARC4. Finally, a third *cya*A-GA expression vector was generated in pSEVA424 from the SEVA collection (Silva-Rocha et al., 2013). In order to construct this plasmid, the *cya*A-GA gene from original pGA15 was excised with SacI/SpeI restriction enzymes and recloned into the same sites of pSEVA424. The resulting broad-host range vector was named pARC5.

Fluorescent measurements in cells transformed with the pCAMPS cAMP-reporter system

A reporter plasmid was constructed to monitor the *in-vivo* production of intracellular cAMP as follows: two complementary oligonucleotides (Supplementary Table S1) were designed to generate a double-stranded DNA (dsDNA) fragment encoding the sequence of the Crp-dependent $P_{CC\text{-}41.5}$ promoter (Gaston et al., 1990). Forward primer aaPCC-5' encodes the leader sequence of $P_{CC\text{-}41.5}$, while reverse primer aaPCC-3' contains the complementary strand for aaPCC-5'. The dsDNA was generated in a hybridization mixture containing 250 mM Tris-HCl pH 7.5 and 20 μM of each oligonucleotide. The reaction was started by 5 min initial denaturation at 95ºC, followed by overnight cooling down. Both complementary oligonucleotides were designed to generate the cohesive ends of the enzymes *EcoRI* and SalI (at 5' and 3' ends, respectively) when hybridizing. Hence, it was possible to clone the $P_{CC\text{-}41.5}$ into the same restriction sites of the promoterless, GFP-reporter vector pSEVA637 (Table 1) to generate the definitive pCAMPS (which stands for cAMP Sensor). Single colonies of *P. putida* KT2440, Δ*cya*A, Δ*crp* and *pde*$^{-}$ transformed with the reporter pCAMPS were picked from fresh LB plates and inoculated into 1 ml of M9 salts medium supplemented with Gm, 0.2% (w/v) of the carbon source indicated in each

case (glucose, fructose or succinate) and 1X trace elements solution (Abril et al., 1989). Overnight growing cells were diluted with the same medium to a low optical density (OD_{600} *ca.* 0.005) and 200 μl of this preparation was used to inoculate a Microtest™ 96-well assay plate (BD Falcon). Cultures were incubated at 30ºC with occasional shaking for 40 hours in the Wallac Victor 2 Microplate Reader (Perkin Elmer, Waltham, MA, USA). At time intervals of 1h, OD_{600} and GFP fluorescence of each culture was measured. The reporter activity was estimated by normalizing the absolute GFP fluorescence to the OD_{600} values. The output of these experiments is the result of at least three biological replicates. To test the sensitivity of the reporter system to extracellular cAMP, single colonies of wild-type or ΔcyaA *E. coli* or *P. putida* strains (as indicated) were grown overnight and used to inoculate 200 μl of M9 salts medium supplemented with Gm, 0.2% (w/v) of the corresponding carbon source (glucose or maltose) and different concentrations of cAMP (where denoted). Cultures were incubated in the Wallac Victor 2 Microplate Reader as described before. GFP fluorescence and OD_{600} were recorded every 15 minutes. Addition of cAMP was done at mid-exponential phase (as indicated) and the reporter activity was normalized to the OD_{600} values. Experiments were done in two technical and three biological replicates.

Quantification of cAMP by HPLC-MS

E. coli and *P. putida* strains were grown on M9 salts medium containing 0.2% (w/v) of the appropriate carbon source until mid-exponential phase (OD_{600} *ca*. 0.5-0.6) in 100-ml Erlenmeyer flasks containing 20 ml of the culture medium. The biomass of a 10-ml culture aliquot was collected by fast centrifugation (14000 rpm, 30 sec, 0ºC), the supernatant was rapidly removed, and the pellet immediately frozen in liquid N_2. cAMP was extracted from cells by vortexing the biomass with 0.5 ml of 10 mM ammonium acetate (pH = 7.2) in 60% (v/v) ethanol at 70°C for 1 min, followed by an incubation for another min at 78°C. The extraction procedure was repeated three times, the supernatants were pooled, and the extract was evaporated to complete dryness in a Speed Vac apparatus at 4ºC. The sediment was kept at -80ºC until analysis and, just before quantification, it was resuspended in 100 μl of milli-Q water. The supernatants of the 10-ml culture aliquots described above were likewise frozen, lyophilized until complete dryness and resuspended in 0.5 ml of milli-Q water. The cAMP concentration in these samples was determined with a Varian Prostar 210 high-performance liquid chromatography system coupled to a Varian 1200L Triple Quadrupole MS (Varian Medical Systems Inc., Palo Alto, California, USA). The Klawitter method was modified as follows. Samples were run on a Zorbax SB-C18 column (150 mm ×

4.6 mm × 5 μm; Agilent Technologies Corp., Santa Clara, California, USA), using a gradient of two phases. Mobile phase I was methanol and phase II consisted in 95% (v/v) of an aqueous buffer (10 mM dibutylamine and 15 mM ammonium acetate) and 5% (v/v) methanol at a flow rate of 0.5 ml/min. The injection volume was 10 μl and the HPLC-ESI-MS analysis was performed in the negative-ion mode. The results of the quantification were obtained in biological duplicates, measured each by three technical replicates.

β-galactosidase assays of lac*Z transcriptional and translational fusions with* cya*A*$_{P.\ putida}$ *promoter*

Reporter plasmids were constructed as follows: a *lac*Z translational fusion of *cya*A promoter was generated by PCR amplification of a 492 bp DNA fragment encompassing 400 bp upstream from ATG start codon plus the DNA sequence codifying the 30 first amino acids (10 codons) of *cya*A. PCR reaction was carried out with oligonucleotides aaPcyaA-F and aaPcyaATrad-R, which includes *EcoRI* and *BamHI* restriction sites respectively. The resulting fragment was digested and cloned into the same sites of pSEVA225T to create pARPcyaA1. Also, a *lac*Z transcriptional fusion of P*cya*A promoter was constructed in order to compare the transcription and translation levels of *cya*A. The DNA fragment for this construct was obtained by PCR amplification of only the 400 bp upstream the *cya*A start codon, using primers aaPcyaA-F (*Eco*RI) and aaPcyaA-R (*Bam*HI). The resulting ~0.4 kb fragment was *EcoRI*/*BamHI* digested and subsequently cloned in vector pSEVA225 previously cleaved with the same restriction nucleases, generating pARPcyaA2. The two plasmids carrying P*cya*A transcriptional and translational fusions were separately transformed in the *P. putida* strains KT2440 wild-type, KT2440 Δ*crp* and KT2440 Δ*cya*A. The β-galactosidase activity of the strains described above was measured by means of the ultra-sensitive Galacto-Light Plus™ commercial system (Applied Biosystems, Foster City, CA, USA). According to the supplier's specifications, this method incorporates a chemiluminiscent substrate for β-galactosidase enzyme and luminescence enhancers that make the system more sensitive to low amounts of enzyme than traditional methods. Briefly, a single colony was grown in 10 ml of M9 salts medium supplemented with Km and 0.2% (w/v) of the appropriate carbon source. When cells reached the exponential phase, 500 μl of the cultures were taken into an Eppendorf tube and spun down by 2 min centrifugation at 14,000 rpm. Cells were resuspended in 200 μl of lysis buffer [100 mM potassium phosphate pH 7.8, 0.2% (v/v) Triton X-100], subjected to two freeze-thaw cycles and centrifuged 1 min at 14.000 rpm to separate cell debris. Then, 20 μl of lysed supernatant were incubated

with 80 µl of reaction buffer (100 mM sodium phosphate pH 8.0, 1 mM $MgCl_2$ and 1X Galacto-Plus® chemiluminiscent substrate) in the dark for 30 minutes, after which 125 µl of Sapphire-II™ light emission accelerator were added. The reactions were incubated 1 min in the dark and the luminescence was recorded in the Wallac Victor 2 Microplate Reader (Perkin Elmer, Waltham, MA, USA). All β-galactosidase measurements are the result of three biological replicates.

Purification of P. putida Crp devoid of cAMP

E. coli W3110 *crp cya*A double mutant was transformed with plasmid pARCrp5, which overexpresses the recombinant MBP-$Crp_{P.\ putida}$ including a thrombin protease cleavage site placed in the linker of both proteins (Arce-Rodriguez et al., 2012). Transformants were inoculated in 800 ml of M9 salts with 0.2% (w/v) glucose (instead of LB medium) and cultured at 37°C to an OD_{600} = 0.5. Next, expression of fusion protein was induced with 0.5 mM IPTG during 2 hours. Cells were spun down and resuspended in 50 mM of sodium phosphate buffer pH 7.0, 200 mM NaCl and 1X of a protease inhibitor cocktail (Roche Applied Science, Mannheim, Germany), followed by disruption in a French press (Thermo Electron corporation, Waltham, MA, USA). Soluble extract was separated from cellular debris by centrifugation and then passed through an amylose-resin column (New England Biolabs, Ipswich, MA, USA). After washing extensively the resin with the same resuspension buffer, the recombinant MBP-Crp fusion protein was eluted with the same buffer containing 10 mM maltose. The MBP-Crp eluted fractions were analyzed by SDS-PAGE, and those which produced an apparently homogeneous protein band were pooled and concentrated in a 50 kDa molecular weight-cutoff centrifugal filter device (Millipore, Billerica, MA, USA). Approximately 12 mg of apo-MBP-Crp were recovered and extensively dialyzed against PBS during 8 hours at 4°C. Prior to cleaving, 0.5 mM DTT was added to the fusion protein, followed by overnight digestion with 240 U of thrombin (Amersham Biosciences) at 22°C. Immediately after cleavage, the protein mixture was passed through 5 ml of PBS-equilibrated P11 phosphocellulose resin column (Whatman) and washed extensively with 80 ml of PBS. Elution of the MBP-free, apo-$Crp_{P.\ putida}$ bound to the phosphocellulose resin was carried out with PBS buffer containing 500 mM KCl. The eluted fractions were pooled, concentrated and dialyzed against 50 mM Na phosphate buffer pH 7.0, 250 mM KCl, 0.67 µM DTT and 20% (v/v) glycerol. The concentration of the protein was calculated to be 0.8 mg/ml as determined by absorbance at 280 nM, using a calculated extinction coefficient of 11.46 x 10^3 M^{-1} cm^{-1} (ProtParam tool, ExPASy server; (Gasteiger et al., 2005).

Isothermal titration calorimetry (ITC) with *purified apo-Crp*$_{P.\ putida}$

Prior to experiments, purified apo-Crp was exhaustively dialyzed in 50 mM K phosphate buffer pH 7.0, 250 mM KCl, 1 mM DTT and 20% (v/v) glycerol. Next, the protein was passed through a 0.22 μm pore size filter device and its concentration was accurately determined by UV absorption spectroscopy. Putative effector molecules were prepared by dissolving the pure compound (cAMP, cGMP or AMP) in the same filtered dialysis buffer described above, in order to homogenize ligand and protein solvent. apo-Crp$_{P.\ putida}$ was diluted to 8-7 μM with the previous buffer and its concentration was accurately calculated by 5 independent measurements of its UV absorption spectroscopy at 280nm. Next, 1.4 ml of protein was titrated in a VP microcalorimeter (MicroCal, Northampton, MA, USA) at 25°C, conducting a first titration with a single 1.6 μl injection of diluted ligands at 200 μM and followed by subsequent injections with 4.8 μl of the same compounds. The mean enthalpies measured from the injection of ligand into buffer were subtracted from the raw titration data, prior to curve fitting using the *One Binding Site* model of the MicroCal (Northampton, MA, USA) version of ORIGIN. From the values obtained for K_A and enthalpy (ΔH), the dissociation constant K_D was determined ($K_D = 1/K_A$) as well as the changes in the free energy (ΔG) and entropy (ΔS) using the equation

$$\Delta G = -RT\ln K_A = \Delta H - T\Delta S$$

where R is the universal molar gas constant and T the absolute temperature.

ACKNOWLEDGEMENTS

To Dr. Mario Mencía for supporting material. To Juhyun Kim for his valuable help in the analysis of RNA-seq transcriptomic data. P.I.N. acknowledges financial support by The Novo Nordisk Foundation (NNF10CC1016517 and NNF18OC0034818) and the Danish Council for Independent Research (SWEET, DFF-Research Project 8021-00039B). Plan Nacional de I+D+I (grant Bio2010-16937) y Plan Estatal de Investigación Científica y Técnica y de Innovación (BIO2016-76779-P). Rosa Sedano. FCE_1_2017_1_136082 y FCE_1_2019_1_156520.

Supplementary Materials

Supplementary Table S1. Oligonucleotides used in this work. Sequences for the corresponding restriction enzymes are underlined.

Supplementary Figure S1. Sequence analysis of *P. putida* PP_4917 gene product compared to other cAMP phosphodiesterases.

Supplementary Figure S2. Overview of the translation initiation region of *P. putida* and *E. coli cya*A genes.

Supplementary Figure S3. Alignment between the DNA sequence of native *cya*A from *P. putida* and its optimized version *cya*A-GA.

Supplementary Figure S4. Model of noise generation in protein expression for a transcriptional unit (e.g. GFP) with (A) low rates of transcription vs high translation, of (B) high transcription vs low levels of translation.

Supplementary Discussion

REFERENCES

Abril, M.A., Michan, C., Timmis, K.N., and Ramos, J.L. (1989) Regulator and enzyme specificities of the TOL plasmid-encoded upper pathway for degradation of aromatic hydrocarbons and expansion of the substrate range of the pathway. J Bacteriol 171: 6782-6790.

Aiba, H. (1985) Transcription of the Escherichia coli adenylate cyclase gene is negatively regulated by cAMP-cAMP receptor protein. J Biol Chem 260: 3063-3070.

Akkaya, O., Perez-Pantoja, D.R., Calles, B., Nikel, P.I., and de Lorenzo, V. (2018) The Metabolic Redox Regime of Pseudomonas putida Tunes Its Evolvability toward Novel Xenobiotic Substrates. mBio 9.

Altschul, S.F., Madden, T.L., Schaffer, A.A., Zhang, J., Zhang, Z., Miller, W., and Lipman, D.J. (1997) Gapped BLAST and PSI-BLAST: a new generation of protein database search programs. Nucleic acids research 25: 3389-3402.

Arce-Rodriguez, A., Durante-Rodriguez, G., Platero, R., Krell, T., Calles, B., and de Lorenzo, V. (2012) The Crp regulator of Pseudomonas putida: evidence of an unusually high affinity for its physiological effector, cAMP. Environmental microbiology 14: 702-713.

Belda, E., van Heck, R.G., José Lopez-Sanchez, M., Cruveiller, S., Barbe, V., Fraser, C. et al. (2016) The revisited genome of Pseudomonas putida KT2440 enlightens its value as a robust metabolic chassis. Environ Microbiol 18: 3403-3424.

Busby, S., and Ebright, R.H. (1999) Transcription activation by catabolite activator protein (CAP). J Mol Biol 293: 199-213.

Choi, K.H., Kumar, A., and Schweizer, H.P. (2006) A 10-min method for preparation of highly electrocompetent Pseudomonas aeruginosa cells: application for DNA fragment transfer between chromosomes and plasmid transformation. Journal of microbiological methods 64: 391-397.

Coggan, K.A., and Wolfgang, M.C. (2012) Global regulatory pathways and cross-talk control pseudomonas aeruginosa environmental lifestyle and virulence phenotype. Curr Issues Mol Biol 14: 47-70.

Cordes, T.J., Worzalla, G.A., Ginster, A.M., and Forest, K.T. (2011) Crystal structure of the Pseudomonas aeruginosa virulence factor regulator. J Bacteriol 193: 4069-4074.

Crasnier, M., and Danchin, A. (1990) Characterization of Escherichia coli adenylate cyclase mutants with modified regulation. Journal of general microbiology 136: 1825-1831.

de Lorenzo, V., and Timmis, K.N. (1994) Analysis and construction of stable phenotypes in gram-negative bacteria with Tn5- and Tn10-derived minitransposons. Methods in enzymology 235: 386-405.

de Lorenzo, V., Eltis, L., Kessler, B., and Timmis, K.N. (1993) Analysis of Pseudomonas gene products using lacIq/Ptrp-lac plasmids and transposons that confer conditional phenotypes. Gene 123: 17-24.

Deutscher, J. (2008) The mechanisms of carbon catabolite repression in bacteria. Curr Opin Microbiol 11: 87-93.

Di Tommaso, P., Moretti, S., Xenarios, I., Orobitg, M., Montanyola, A., Chang, J.M. et al. (2011) T-Coffee: a web server for the multiple sequence alignment of protein and RNA sequences using structural information and homology extension. Nucleic acids research 39: W13-17.

Duque, E., Molina-Henares, A.J., Torre, J.d.l., Molina-Henares, M.A., Castillo, T.d., Lam, J., and Ramos, J.L. (2007) Towards a Genome-Wide Mutant Library of Pseudomonas putida Strain KT2440

Pseudomonas. In. Ramos, J.-L., and Filloux, A. (eds): Springer Netherlands, pp. 227-251.

Fahrner, K.A., and Berg, H.C. (2015) Mutations That Stimulate flhDC Expression in Escherichia coli K-12. J Bacteriol 197: 3087-3096.

Fuchs, E.L., Brutinel, E.D., Klem, E.R., Fehr, A.R., Yahr, T.L., and Wolfgang, M.C. (2010) In vitro and in vivo characterization of the Pseudomonas aeruginosa cyclic AMP (cAMP) phosphodiesterase CpdA, required for cAMP homeostasis and virulence factor regulation. J Bacteriol 192: 2779-2790.

Gancedo, J.M. (2013) Biological roles of cAMP: variations on a theme in the different kingdoms of life. Biol Rev Camb Philos Soc 88: 645-668.

Gasteiger, E., Hoogland, C., Gattiker, A., Duvaud, S.e., Wilkins, M., Appel, R., and Bairoch, A. (2005) Protein Identification and Analysis Tools on the ExPASy Server. In The Proteomics Protocols Handbook. Walker, J. (ed): Humana Press, pp. 571-607.

Gaston, K., Bell, A., Kolb, A., Buc, H., and Busby, S. (1990) Stringent spacing requirements for transcription activation by CRP. Cell 62: 733-743.

Gorshkova, I., Moore, J.L., McKenney, K.H., and Schwarz, F.P. (1995) Thermodynamics of cyclic nucleotide binding to the cAMP receptor protein and its T127L mutant. J Biol Chem 270: 21679-21683.

Green, J., Stapleton, M.R., Smith, L.J., Artymiuk, P.J., Kahramanoglou, C., Hunt, D.M., and Buxton, R.S. (2014) Cyclic-AMP and bacterial cyclic-AMP receptor proteins revisited: adaptation for different ecological niches. Curr Opin Microbiol 18: 1-7.

Hanahan, D., and Meselson, M. (1983) Plasmid screening at high colony density. Methods Enzymol 100: 333-342.

Herrera, M.C., Daddaoua, A., Fernandez-Escamilla, A., and Ramos, J.L. (2012) Involvement of the global Crp regulator in cyclic AMP-dependent utilization of aromatic amino acids by Pseudomonas putida. J Bacteriol 194: 406-412.

Hufnagel, D.A., Evans, M.L., Greene, S.E., Pinkner, J.S., Hultgren, S.J., and Chapman, M.R. (2016) The Catabolite Repressor Protein-Cyclic AMP Complex Regulates csgD and Biofilm Formation in Uropathogenic Escherichia coli. J Bacteriol 198: 3329-3334.

Jaenecke, S., and Diaz, E. (1999) Construction of plasmid vectors bearing a NotI-expression cassette based on the lac promoter. International microbiology : the official journal of the Spanish Society for Microbiology 2: 29-31.

Jelesarov, I., and Bosshard, H.R. (1999) Isothermal titration calorimetry and differential scanning calorimetry as complementary tools to investigate the energetics of biomolecular recognition. J Mol Recognit 12: 3-18.

Joseph, E., Bernsley, C., Guiso, N., and Ullmann, A. (1982) Multiple regulation of the activity of adenylate cyclase in Escherichia coli. Mol Gen Genet 185: 262-268.

Kaern, M., Elston, T.C., Blake, W.J., and Collins, J.J. (2005) Stochasticity in gene expression: from theories to phenotypes. Nat Rev Genet 6: 451-464.

Kessler, B., de Lorenzo, V., and Timmis, K.N. (1992) A general system to integrate lacZ fusions into the chromosomes of gram-negative eubacteria: regulation of the Pm promoter of the TOL plasmid studied with all controlling elements in monocopy. Mol Gen Genet 233: 293-301.

Lin, S.H., and Lee, J.C. (2002) Communications between the high-affinity cyclic nucleotide binding sites in E. coli cyclic AMP receptor protein: effect of single site mutations. Biochemistry 41: 11857-11867.

Ma, J., Campbell, A., and Karlin, S. (2002) Correlations between Shine-Dalgarno sequences and gene features such as predicted expression levels and operon structures. J Bacteriol 184: 5733-5745.

Makman, R.S., and Sutherland, E.W. (1965) Adenosine 3',5'-Phosphate in Escherichia Coli. J Biol Chem 240: 1309-1314.

Manoil, C., and Beckwith, J. (1985) TnphoA: a transposon probe for protein export signals. Proc Natl Acad Sci U S A 82: 8129-8133.

Martinez-Garcia, E., and de Lorenzo, V. (2011) Engineering multiple genomic deletions in Gram-negative bacteria: analysis of the multi-resistant antibiotic profile of Pseudomonas putida KT2440. Environmental microbiology 13: 2702-2716.

McDonough, K.A., and Rodriguez, A. (2011) The myriad roles of cyclic AMP in microbial pathogens: from signal to sword. Nat Rev Microbiol 10: 27-38.

Milanesio, P., Arce-Rodriguez, A., Munoz, A., Calles, B., and de Lorenzo, V. (2011) Regulatory exaptation of the catabolite repression protein (Crp)-cAMP system in Pseudomonas putida. Environ Microbiol 13: 324-339.

Miller, J.H. (1972) Experiments in molecular genetics. New York: Cold Spring Harbor Laboratory.

Milligan, D.L., and Koshland, D.E., Jr. (1993) Purification and characterization of the periplasmic domain of the aspartate chemoreceptor. J Biol Chem 268: 19991-19997.

Molina-Quiroz, R.C., Silva-Valenzuela, C., Brewster, J., Castro-Nallar, E., Levy, S.B., and Camilli, A. (2018) Cyclic AMP Regulates Bacterial Persistence through Repression of the Oxidative Stress Response and SOS-Dependent DNA Repair in Uropathogenic Escherichia coli. mBio 9.

Moreno, R., Hernandez-Arranz, S., La Rosa, R., Yuste, L., Madhushani, A., Shingler, V., and Rojo, F. (2015) The Crc and Hfq proteins of Pseudomonas putida cooperate in catabolite repression and formation of ribonucleic acid complexes with specific target motifs. Environ Microbiol 17: 105-118.

Mori, K., and Aiba, H. (1985) Evidence for negative control of cya transcription by cAMP and cAMP receptor protein in intact Escherichia coli cells. J Biol Chem 260: 14838-14843.

Nelson, K.E., Weinel, C., Paulsen, I.T., Dodson, R.J., Hilbert, H., Martins dos Santos, V.A. et al. (2002) Complete genome sequence and comparative analysis of the metabolically versatile Pseudomonas putida KT2440. Environmental microbiology 4: 799-808.

Nikel, P.I., and de Lorenzo, V. (2018) Pseudomonas putida as a functional chassis for industrial biocatalysis: From native biochemistry to trans-metabolism. Metab Eng 50: 142-155.

Nikel, P.I., Kim, J., and de Lorenzo, V. (2013) Metabolic and regulatory rearrangements underlying glycerol metabolism in Pseudomonas putida KT2440. Environmental microbiology.

Nikel, P.I., Chavarria, M., Fuhrer, T., Sauer, U., and de Lorenzo, V. (2015) Pseudomonas putida KT2440 Strain Metabolizes Glucose through a Cycle Formed by Enzymes of the Entner-Doudoroff, Embden-Meyerhof-Parnas, and Pentose Phosphate Pathways. J Biol Chem 290: 25920-25932.

Ozbudak, E.M., Thattai, M., Kurtser, I., Grossman, A.D., and van Oudenaarden, A. (2002) Regulation of noise in the expression of a single gene. Nat Genet 31: 69-73.

Passner, J.M., and Steitz, T.A. (1997) The structure of a CAP-DNA complex having two cAMP molecules bound to each monomer. Proc Natl Acad Sci U S A 94: 2843-2847.

Perez-Martin, J., and de Lorenzo, V. (1996) VTR expression cassettes for engineering conditional phenotypes in Pseudomonas: activity of the Pu promoter of the TOL plasmid under limiting concentrations of the XylR activator protein. Gene 172: 81-86.

Phillips, A.T., and Mulfinger, L.M. (1981) Cyclic adenosine 3',5'-monophosphate levels in Pseudomonas putida and Pseudomonas aeruginosa during induction and carbon catabolite repression of histidase synthesis. J Bacteriol 145: 1286-1292.

Popovych, N., Sun, S., Ebright, R.H., and Kalodimos, C.G. (2006) Dynamically driven protein allostery. Nat Struct Mol Biol 13: 831-838.

Rodgers, T.L., Townsend, P.D., Burnell, D., Jones, M.L., Richards, S.A., McLeish, T.C. et al. (2013) Modulation of global low-frequency motions underlies allosteric regulation: demonstration in CRP/FNR family transcription factors. PLoS Biol 11: e1001651.

Rojo, F. (2010) Carbon catabolite repression in Pseudomonas : optimizing metabolic versatility and interactions with the environment. FEMS Microbiol Rev 34: 658-684.

Sambrook, J., Fritsch, E.F., and Maniatis, T. (1989) Molecular cloning: A laboratory manual. New York: Cold Spring Harbor Laboratory.

Seok, S.H., Im, H., Won, H.S., Seo, M.D., Lee, Y.S., Yoon, H.J. et al. (2014) Structures of inactive CRP species reveal the atomic details of the allosteric transition that discriminates cyclic nucleotide second messengers. Acta Crystallogr D Biol Crystallogr 70: 1726-1742.

Shimada, T., Fujita, N., Yamamoto, K., and Ishihama, A. (2011) Novel roles of cAMP receptor protein (CRP) in regulation of transport and metabolism of carbon sources. PLoS One 6: e20081.

Silva-Rocha, R., Martinez-Garcia, E., Calles, B., Chavarria, M., Arce-Rodriguez, A., de Las Heras, A. et al. (2013) The Standard European Vector Architecture (SEVA): a coherent platform for the analysis and deployment of complex prokaryotic phenotypes. Nucleic acids research 41: D666-675.

Stapleton, M., Haq, I., Hunt, D.M., Arnvig, K.B., Artymiuk, P.J., Buxton, R.S., and Green, J. (2010) Mycobacterium tuberculosis cAMP receptor protein (Rv3676) differs from the Escherichia coli paradigm in its cAMP binding and DNA binding properties and transcription activation properties. J Biol Chem 285: 7016-7027.

Teran, W., Krell, T., Ramos, J.L., and Gallegos, M.T. (2006) Effector-repressor interactions, binding of a single effector molecule to the operator-bound TtgR homodimer mediates derepression. J Biol Chem 281: 7102-7109.

Topal, H., Fulcher, N.B., Bitterman, J., Salazar, E., Buck, J., Levin, L.R. et al. (2012) Crystal structure and regulation mechanisms of the CyaB adenylyl cyclase from the human pathogen Pseudomonas aeruginosa. J Mol Biol 416: 271-286.

Townsend, P.D., Jungwirth, B., Pojer, F., Bussmann, M., Money, V.A., Cole, S.T. et al. (2014) The crystal structures of apo and cAMP-bound GlxR from Corynebacterium glutamicum reveal structural and dynamic changes upon cAMP binding in CRP/FNR family transcription factors. PLoS One 9: e113265.

Townsend, P.D., Rodgers, T.L., Glover, L.C., Korhonen, H.J., Richards, S.A., Colwell, L.J. et al. (2015) The Role of Protein-Ligand Contacts in Allosteric Regulation of the Escherichia coli Catabolite Activator Protein. J Biol Chem 290: 22225-22235.

Trotot, P., Sismeiro, O., Vivares, C., Glaser, P., Bresson-Roy, A., and Danchin, A. (1996) Comparative analysis of the cya locus in enterobacteria and related gram-negative facultative anaerobes. Biochimie 78: 277-287.

Ullmann, A., and Monod, J. (1968) Cyclic AMP as an antagonist of catabolite repression in Escherichia coli. FEBS Lett 2: 57-60.

Weber, I.T., and Steitz, T.A. (1987) Structure of a complex of catabolite gene activator protein and cyclic AMP refined at 2.5 A resolution. J Mol Biol 198: 311-326.

Wirth, R., Friesenegger, A., and Fiedler, S. (1989) Transformation of various species of gram-negative bacteria belonging to 11 different genera by electroporation. Molecular & general genetics : MGG 216: 175-177.

Wong, S.M., and Mekalanos, J.J. (2000) Genetic footprinting with mariner-based transposition in Pseudomonas aeruginosa. Proceedings of the National Academy of Sciences of the United States of America 97: 10191-10196.

Xiao, Y., Liu, H., He, M., Nie, L., Nie, H., Chen, W., and Huang, Q. (2020) A crosstalk between c-di-GMP and cAMP in regulating transcription of GcsA, a diguanylate cyclase involved in swimming motility in Pseudomonas putida. Environ Microbiol 22: 142-157.

Xue, J., Tan, B., Yang, S., Luo, M., Xia, H., Zhang, X. et al. (2016) Influence of cAMP receptor protein (CRP) on bacterial virulence and transcriptional regulation of allS by CRP in Klebsiella pneumoniae. Gene 593: 28-33.

Yang, D., Wang, Z., Ma, J., Fu, Q., Wu, L., Wang, H. et al. (2020) Glycine Cleavage System and cAMP Receptor Protein Co-Regulate CRISPR/cas3 Expression to Resist Bacteriophage. Viruses 12.

Yanisch-Perron, C., Vieira, J., and Messing, J. (1985) Improved M13 phage cloning vectors and host strains: nucleotide sequences of the M13mp18 and pUC19 vectors. Gene 33: 103-119.

Yuste, L., Hervas, A.B., Canosa, I., Tobes, R., Jimenez, J.I., Nogales, J. et al. (2006) Growth phase-dependent expression of the Pseudomonas putida KT2440 transcriptional machinery analysed with a genome-wide DNA microarray. Environ Microbiol 8: 165-177.

Table 1. Strains and plasmids used in this work.

Strain/plasmid	Description / relevant characteristics	Reference
E. coli strains		
CC118	F$^-$, Δ(*ara-leu*)7697, *ara*D139, Δ(*lac*)X74, *pho*AΔ20, *gal*E, *gal*K, *thi*, *rps*E, *rpo*B, *arg*E(Am), *rec*A1	(Manoil and Beckwith, 1985)
DH5α	F$^-$, *sup*E44, Δ*lac*U169, (ϕ80 *lac*ZDM15), *hsd*R17, (rk$^-$ mk$^+$), *rec*A1, *end*A1, *thi*1, *gyr*A, *rel*A	(Hanahan and Meselson, 1983)
JM109	F´, *tra*D36, *pro*A$^+$B$^+$, *lac*I^q, Δ(*lac*Z)M15 Δ(*lac-pro*AB), *gln*V44 *e14*$^-$, *gyr*A96, *rec*A1, *rel*A1, *end*A1, *thi*, *hsd*R17	(Yanisch-Perron et al., 1985)
DH5αλ*pir*	λ*pir* phage lysogen of DH5α	Lab collection
HB101	Sm^R, *hsd*R-M+, *pro*, *leu*, *thi*, *rec*A	(Sambrook et al., 1989)
W3110 *cyaA*	Prototrophic, F$^-$, I$^-$, IN (*rrn*D-*rrn*E)1, *rph*-1; *cya*A deletion derivative of W3110 strain	(Milanesio et al., 2011)
W3110 *crp cyaA*	Prototrophic, F$^-$, I$^-$, IN (*rrn*D-*rrn*E)1, *rph*-1; *crp* and *cya*A double mutant	(Milanesio et al., 2011)
TP610A	F$^-$, *thi*-1, *thr*-1, *leu*B6, *pro*, *lac*Y1, *ton*A2I, *sup*E44, λ-*hsd*R *hsd*M *rec*BC *lop*-11 *lig*$^+$ *cya*-610; spontaneous mutant of strain TP610 with hypersensitivity to low levels of cAMP	(Crasnier and Danchin, 1990)
P. putida strains		
KT2440	*rsd*R; prototrophic, wild-type strain derived of *P. putida* mt-2 without pWWO plasmid	(Nelson et al., 2002)
KT2440 Δ*crp*	KT2440 derivative with a full deletion of *crp*	This work
KT2440 Δ*cya*A	KT2440 derivative with a full deletion of *cya*A	This work
KT2440 *pde*$^-$	Km^R, Rif^R; KT2440 derivative carrying a chromosomal insertion of a miniTn5-Km in locus PP_4917 (*pde*)	(Duque et al., 2007)

Plasmids		
pRK600	Cm^R, *oriV* ColE1, *tra*$^+$*mob*$^+$ of RK2; helper plasmid for mobilization in tripartite conjugations	(Kessler et al., 1992)
pEMG	Km^R, *oriV* R6K, *lac*Zα with two flanking I-*Sce*I sites Cm^R, Km^R, Ap^R, Sm, Gm, Tc	(Martinez-Garcia and de Lorenzo, 2011)
pARCrp9	Km^R, suicide pEMG carrying the upstream and downstream flanking regions of *P. putida crp* gene	This work
pJΔcyaA	Km^R, suicide pEMG carrying the upstream and downstream flanking regions of *P. putida cya*A gene	This work
pSW-1	Ap^R, *oriV* RK2, *xylS*, bearing a *Pm*→*I-sce*I transcriptional fusion	(Wong and Mekalanos, 2000)
pGA15cyaA-GA	Km^R, *oriV* ColE1, *lac*Zα, pGA15 cloned with the optimized version of *P. putida cya*A (*cya*A-GA)	This work
pVTR-A	Cm^R, *oriV* PSC101, LacIq/IPTG inducible expression cassette inserted as a *Not*I segment	(Perez-Martin and de Lorenzo, 1996)
pARC1	Cm^R, pVTR-A cloned in frame with *cya*A-GA gene from pGA15cyaA-GA	This work
pSJ33	Km^R, *oriV* RSF1010, P_{lac}, *lac*Zα	(Jaenecke and Diaz, 1999)
pARC4	Km^R, pSJ33 bearing the *Not*I fragment from pARC1 which includes the expression cassette for *cya*A-GA	This work
pSEVA424	Sm/Sp^R, *oriV* RK2, *oriT*, *lac*I^q/P_{trc} expression cassette	(Silva-Rocha et al., 2013)
pARC5	Sm/Sp^R, pSEVA424 bearing the expression of *cya*A-GA optimized gene	This work
pSEVA637	Gm^R, *oriV* pBBR1, *oriT*, promoter-less cloning vector including the *gfp* as a reporter gene	(Silva-Rocha et al., 2013)

pCAMPS	Gm^R, pSEVA637 cloned with the sequence of $P_{CC-41.5}$ artificial promoter	This work
pARCrp5	Ap^R, pMAL-C2T overexpression vector harboring the MBP-Crp fusion protein	(Arce-Rodriguez et al., 2012)
pARC2	Cm^R, pVTR-A with its *Not*I insert altogether replaced by a segment bearing the *cya*A gene of *E. coli* expressed through its native transcription and translation signals.	(Milanesio et al., 2011)
pVLT31	Tc^R, *oriV* RSF1010, broad-host range LacIq/IPTG inducible expression vector	(de Lorenzo et al., 1993)
pMZC5	Tc^R, pVLT31 inserted with the *P. putida* native *cya*A gene sequence	(Milanesio et al., 2011)
pSEVA225T	Km^R, *oriV* RK2, *oriT*, promoter-less cloning vector for translational fusions with *lac*Z	(Silva-Rocha et al., 2013)
pARPcyaA1	Km^R, pSEVA225T harboring a P_{cyaA}→*cya*A'-'*lac*Z translational fusion	This work
pSEVA225	Km^R, *oriV* RK2, *oriT*, promoter-less cloning vector for transcriptional fusions with *lac*Z	(Silva-Rocha et al., 2013)
pARPcyaA2	Km^R, pSEVA225 harboring a translational fusion of P_{cyaA} with *lac*Z	This work

1
2

Table 2. Thermodynamic parameters obtained from titration of apo-Crp*P. putida* with putative effectors.

Ligand	Stoichiometry	K_A (M^{-1})	K_D	ΔH (kcal/mol)	$T\Delta S$ (kcal/mol)	ΔG (kcal/mol)
MBP-Crp*P. putida* [a]						
cAMP	0.65 ± 0.01	(4.4 ± 0.5) x 10^7	22.5 ± 2.8 nM	-5.97 ± 0.03	4.47 ± 0.1	-10.44 ± 0.1
cGMP	0.49 ± 0.02	(3.9 ± 0.4) x 10^5	2.6 ± 0.3 μM	-4.16 ± 0.27	3.46 ± 0.3	-7.62 ± 0.06
AMP	*nd* [b]					
apo-Crp*P. putida*						
cAMP	0.498 ± 0.002	(2.2 ± 0.2) x 10^7	45.0 ± 3.4 nM	-4.89 ± 0.03	5.11 ± 0.05	-10.0 ± 0.1
cGMP	0.327 ± 0.084	(1.7 ± 0.2) x 10^5	5.7 ± 0.7 μM	-15.24 ± 4.3	-8.09 ± 4.3	-7.15 ± 0.07

[a]. Data obtained from (Arce-Rodriguez et al., 2012)

[b]. No binding was observed for non-cyclic AMP

FIGURES

Fig. 1. Genomic context and expression profiles of the 3 constituents of the *pde/crp/cyaA* regulatory device.

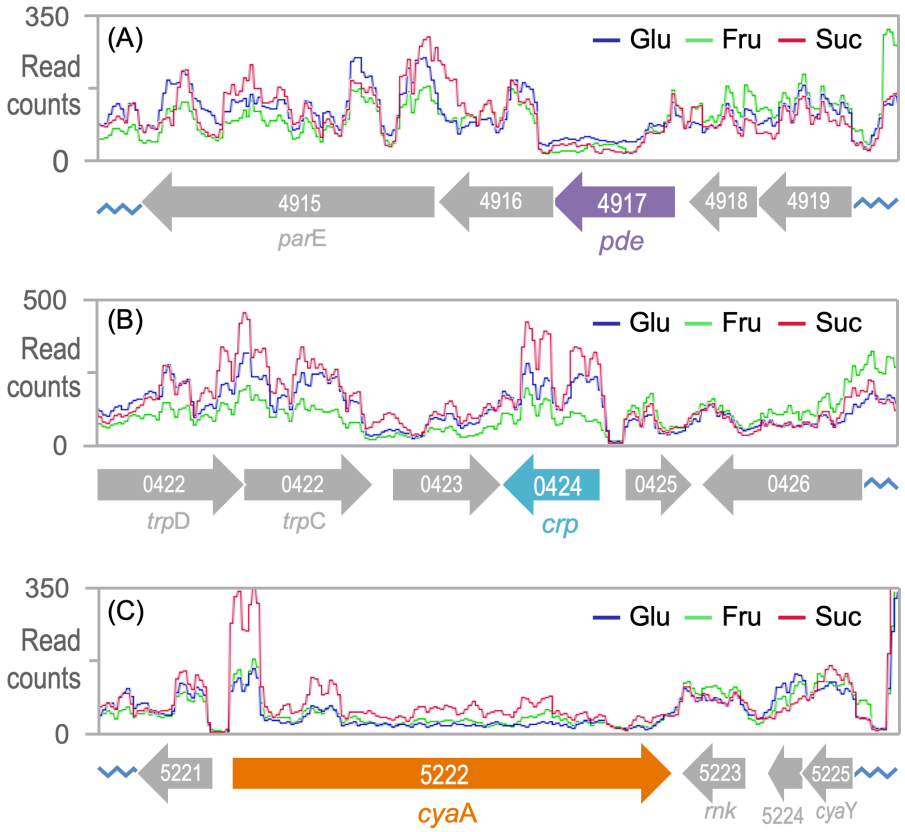

Expression patterns of genes *pde* (called formerly *cpd*A) encoding 3',5'-cyclic-nucleotide phosphodiesterase **(A)**, *crp for the* cAMP regulatory protein **(B)** and *cya*A, adenylate cyclase **(C)** in *Pseudomonas putida* KT2440 analysed by RNA-seq deep sequencing transcriptomics are shown aligned with their respective genomic locations and the code for their PP numbers. Panels show the sequence coverage plots for samples taken during mid-log phase from cultures grown on M9 salts with succinate, glucose or fructose as the sole C source as indicated in the conditions described in (Nikel et al., 2013)]. The representative region shown below the plot charts represent the genome context surrounding each gene. Note that expression of the three genes does not change significantly respective to the carbon source. Also, note the low expression of all genes, specially *pde* and *cya*A.

Fig. 2. Role of *crp, cyaA* and *pde* genes on the activity of the (cAMP-Crp)-dependent $P_{CC(-41.5)}$ promoter in exponential and stationary phase of growth.

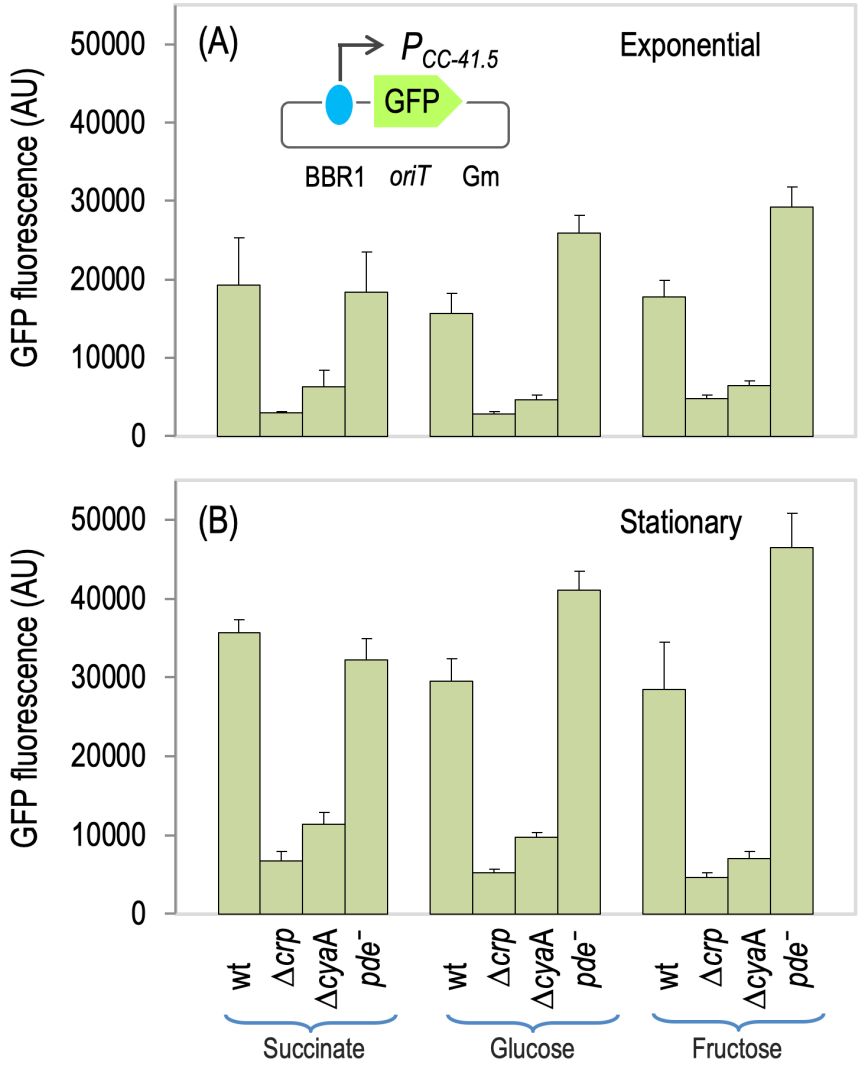

The functional parts of the reporter plasmid pCAMPS (sketched an insert in the upper panel) include an BBR1 origin of replication, a transcriptional fusion between the synthetic Crp-responsive promoter $P_{CC(-41.5)}$, a marker gene for gentamicin resistance (Gm) and an origin of transfer (*oriT*). pCAMPS was transformed in wild type *P. putida* KT2440 and its derived Δ*crp*, Δ*cya*A and *pde*⁻ mutants. These strains were inoculated in M9 salts supplemented with succinate, glucose or fructose as the only carbon source and grown at 30°C in microtiter plates. The OD_{600} and the GFP specific fluorescence were flowed each hour in a Victor 2 multireader and values at mid-exponential phase (A) or stationary phase (B) measured as shown. The basal fluorescence endowed by the promoterless vector (pSEVA637) was subtracted in all cases. The experiment was carried out at least in triplicate.

Fig. 3. Quantification of the cAMP production in **(A)** *E. coli* and **(B-C)** *P. putida* cells grown in different carbon sources.

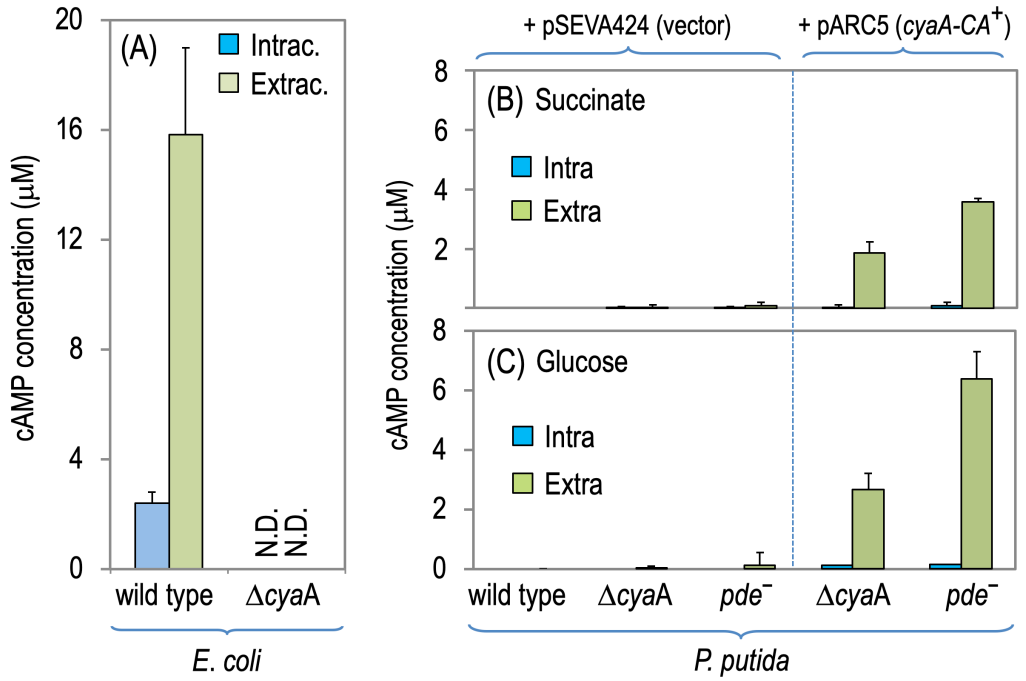

Note that *E. coli* W3110 was cultured in succinate as carbon source, while its Δ*cya*A mutant was grown in glucose (see text for details). The levels of cAMP were determined in both cells and supernatants of wild-type *E. coli* and *P. putida* strains, along with some mutants of the cAMP-Crp system, as explained in Experimental Procedures. The maximum cAMP levels in *P. putida* were induced by the expression of the optimized CyaA-GA protein borne in plasmid pARC5.

Figure 4. The *cya*A gene of *P. putida* is transcribed efficiently, but it is poorly translated into its corresponding protein.

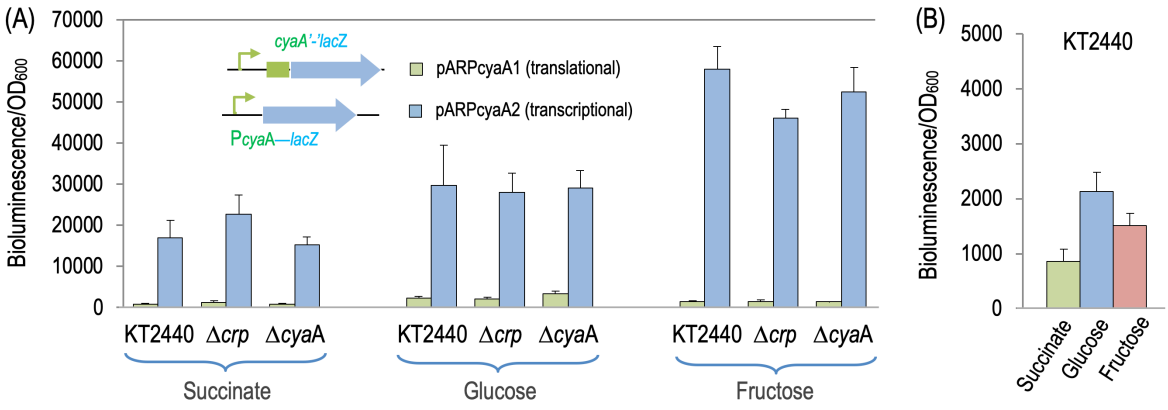

(A) β-galactosidase activity of translational (green) and transcriptional (blue) fusions of P_{cyaA} promoter with *lac*Z gene. Plasmids encoding the promoter fusions were transferred to the indicated *P. putida* hosts and the enzymatic activity was measured by the Galacto-Light Plus™ method in cultures grown on succinate, glucose or fructose as the only carbon source. The basal level of promoter-less plasmids (pSEVA225T and pSEVA225) was respectively subtracted from measured LacZ activity. The experiment was run on triplicates. **(B)** Zoom-in of the β-galactosidase activity in *P. putida* KT2440 bearing the translational fusion of P_{cyaA} (pARPcyaA1) grown in 3 different carbon sources, as depicted in (A). Note the change in the scale of the y-axis.

Fig. 5. Qualitative comparison of the cAMP content in *E. coli cya*A-deficient cells harboring the native *cya*A of *P. putida* and its optimized counterpart (*cya*A-GA).

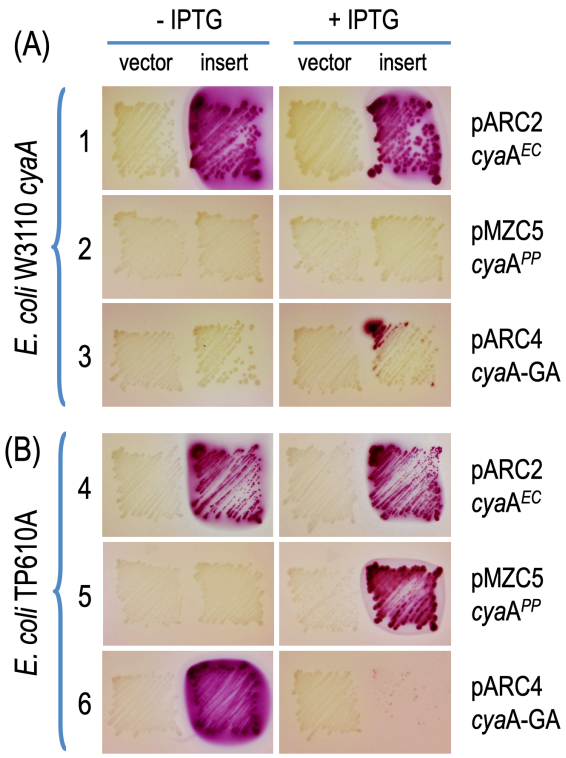

E. coli Δ*cya*A and the cAMP-hypersensitive TP610A strain were transformed with two plasmids bearing the indigenous *cya*A$_{P.\ putida}$ gene or its optimized version (*cya*A-GA) in which the codon usage, the translation initiation region and other features were modified to improve its translation (see Experimental procedures for details). The cAMP production was correlated with the rescue of Mal+ phenotype (red-colored colonies) in MacConkey Agar plates. Note the toxicity of overexpressing the *cya*A-GA in the hypersensitive TP610A *E. coli* strain, which inhibits growth of the corresponding cells.

Fig. 6. Effect of the addition of extracellular cAMP to *cya*A defective strains of *E. coli* and *P. putida*.

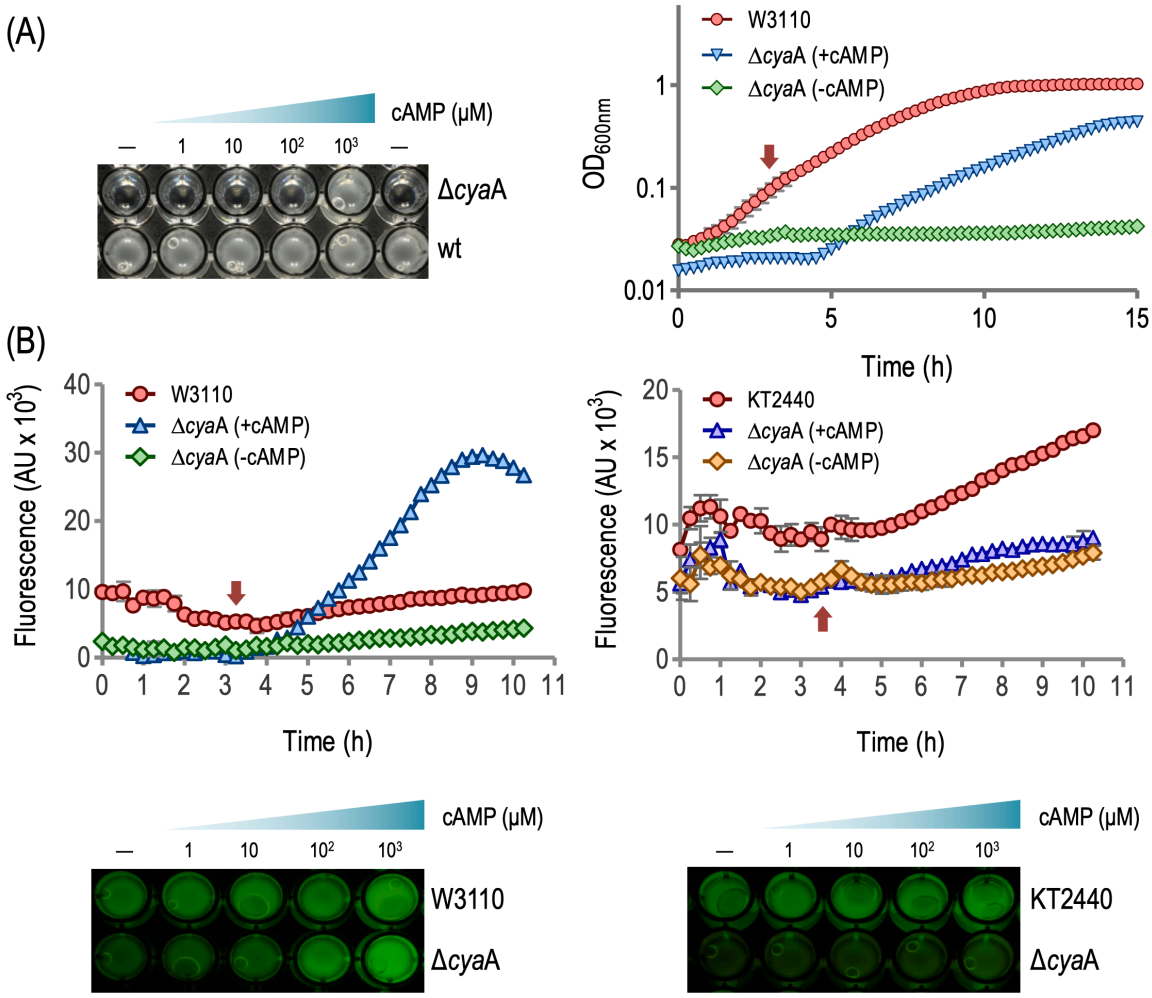

(A) Microtiter plate (left panel) containing cultures of *E. coli* W3110 and its *cya*A derivative after 20 hours of growth in minimal M9 salts with maltose as sole carbon source. The addition of increasing concentrations of cAMP is indicated. The right panel shows the corresponding growth curves of the same strains cultured with (1 mM) or without cAMP. Addition of cAMP (where indicated) was made in the mid-exponential growth phase and the time point is denoted with a red arrow (usually after 3h of growth). **(B)** cAMP-dependent GFP expression from the pCAMPS reporter plasmid transformed in wild-type and *cya*A strains of *E. coli* (upper-left panel) and *P. putida* (upper-right panel). Cells were grown in M9 salts supplemented with glucose as sole carbon source, in the presence (1 mM) or in the absence of cAMP. The cAMP addition is denoted with a red arrow and usually took place between 3 and 4 hours after inoculation, when the cultures reached the mid-exponential phase. The lower panels show final GFP levels reached after 20 hours of growth by adding increasing concentrations of cAMP in *E. coli* (left) and *P. putida* (right).

Fig. 7. Isothermal titration microcalorimetry of apo-Crp$_{P.\ putida}$ interacting with **(A)** cAMP and **(B)** cGMP.

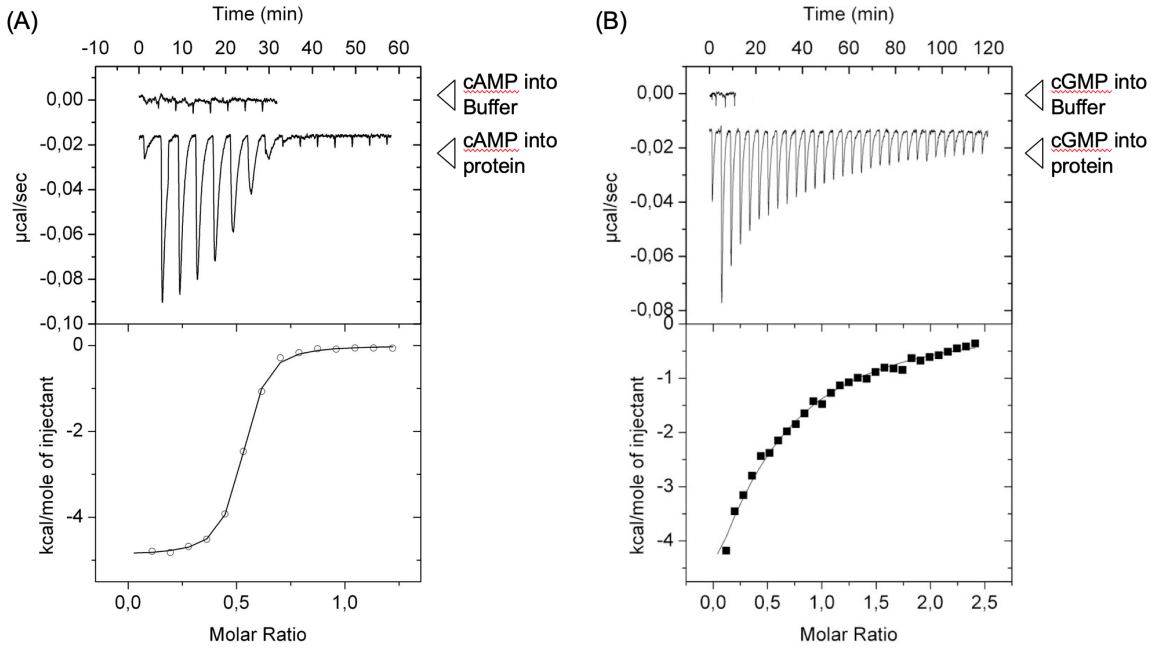

The upper panels plot the raw data obtained from titrations with the cyclic nucleotides. The first titration in these panels exhibits the injection of the effector molecule into buffer without protein. The lower panels represent the integrated and dilution-corrected curves fitted from raw data with the One Binding Site model of the MicroCal version of ORIGIN software. Thermodynamic parameters obtained from curves are summarized in Table 2.